

# On the chaotic dynamic response of deterministic nonlinear single and multi-degree-of-freedom systems<sup>†</sup>

S. K. A. Shah, A. Soleiman Fallah<sup>\*</sup> and L. A Louca

*Department of Civil and Environmental Engineering, South Kensington Campus, Imperial College London, London SW7 2AZ, UK*

(Manuscript Received October 12, 2011; Revised January 31, 2012; Accepted February 17, 2012)

## Abstract

This paper presents a comprehensive study on counter-intuitive or chaotic dynamic response of prototype discrete parameter models of single or multiple degrees of freedom subject to blast or impact loading. Non-linear dynamic behaviour of a typical single degree-of-freedom (SDOF) and multi-degree-of-freedom (MDOF) systems are studied by taking into account cubic and quintic non-linearities, elastic perfect-plastic, and elastic-plastic-hardening and softening behaviours. The first part is founded on Duffing's equation and Ueda's work on strange attractors which indicates the presence of chaos in deterministic systems by using chaos detection techniques such as Poincare's mapping and Lyapunov's exponents and in some cases by fractal dimensions. In these deterministic problems, the system hesitates to settle between two different possible settling regimes despite the fact that the input parameters to the system are deterministic. In a SDOF model with elastic perfectly-plastic or elastic-plastic-hardening resistance function the sign of the permanent plastic deformation may or may not coincide with that of loading direction hence chaotic behaviour can be observed. For an elastic-plastic-softening system, subjected to blast loading, the problem is sensitive to the ratio of post yield stiffness to initial stiffness and for certain ranges of this parameter a small change can replicate into an abrupt change in response. Examples are included of finite elements models with many degrees of freedom of beams and plates. As most intricate engineering structures are composed of these structural elements the existence of component chaos can imply global counter-intuitive behaviour.

**Keywords:** Chaos; Counter-intuitive response; Discrete parameter model; Dynamic loading; Non-linearity; SDOF and MDOF systems

## 1. Introduction

Non-linear dynamical systems are encountered in many problems in the fields of science and engineering. From large amplitude vibration of a pendulum in structural and mechanical engineering to heart beats in medical sciences and from predication of planetary motion of celestial objects in astronomy to the predication of weather in meteorology as well as to animal population growth problem in biology. Henry Poincare was the pioneer of the field and is, rightfully, named the founder of non-linear dynamics. For some, the study of dynamics started and ended with Newton's second law of motion ( $\Sigma F = ma$ ). It was believed that if the nature of forces between the particles and their initial positions and velocities are known, one could predict the motion or history of a system forever. But there exist mechanical systems, whose parameters are all deterministic, yet their final motion is unpredictable as some non-linear systems hesitate to settle between the two final motions. Such non-linear systems are sensitive to initial

conditions and slight perturbations in these conditions can induce utterly different futures.

Counter-intuitive response in structural engineering was first observed by Galiev [1] in 1970s. In his experiments, discs made up of different metals covering a circular hole in the thick wall of a tank were subjected to shock pressure pulses produced by detonating an explosive charge underwater. Permanent outward deflection was a common observation. But in one set of experiments when the pressure was increased in steps, at certain point the final deflection was inward, contrary to intuition. He concluded that the negative pressure behind the compressive shock front and cavitations in the test conducted in water are mainly responsible for inward permanent deflection of discs [1-3].

Independently, similar counter-intuitive response was observed numerically, when a beam was subjected to impact/blast load, by Symonds [4]. After the peak deflections were reached, there was a 'recovery' phase which initially involved elastic unloading. In turn, that resulted eventually to elastic vibrations. After these vibrations were damped out the structure was left in a state of permanent deformation and residual stresses.

Following the same observed phenomenon of counter-

<sup>\*</sup>Corresponding author. Tel.: +44(0) 20 7594 6028, Fax.: +44(0) 20 7594 5934  
E-mail address: arash.soleiman-fallah@imperial.ac.uk

<sup>†</sup>Recommended by Associate Editor Jun Sik Kim

© KSME & Springer 2012

intuitive behaviour by Symonds, research has been reported to validate it experimentally, analytically and numerically [5-9]. A number of research works have also been reported on the existence of counter-intuitive or chaotic behaviour in other types of structural elements e.g. plates, shells, elastic cable, etc. and on mathematical evidence of chaotic solution in second order non-linear differential equations in literature [9-14]. For some structural elements (bars, plates and shallow shells) it is found that within certain ranges of the loading parameters, it may be impossible to predict the response behaviour. This occurs because, for these structural elements, which obey non-linear equations of motion, there may be an extreme sensitivity to changes to these loading parameters in some ranges. Actual values are known in practice only within a tolerance limit and the behaviour must be regarded as unpredictable. This phenomenon occurs typically in the ranges associated with the transition of response from purely elastic to mixed elastic and plastic [2].

In the case of SDOF systems with large deflections, it is unavoidable to include cubic and quintic terms in the governing equation of motion; chaos can be detected qualitatively by observing phase space portrait of the system i.e. the plot of displacement vs. velocity with velocity taken as ordinate conventionally and displacement as abscissa, and quantitatively by calculating Lyapunov's exponent of motion for the system which portrays whether the two systems, exactly the same in defining parameters but one with slightly perturbed initial conditions are converging to a single point (also called point attractor) or diverging from one another with time (also called Chaos). Phase space is an abstract mathematical space spanned over the dynamical variables of the system. The state of dynamical system at a given instant in time can be represented by a point in this phase space. Lyapunov's exponent is widely used for almost all initial conditions in a bounded dynamical system and is the criterion for deterministic chaos [15]. When a damped linear SDOF system is subjected to dynamic loading, the system starts vibrations and with time when the loading stage completes, the motion is damped out gradually depending upon the damping mechanisms associated with the motion and finally settles down to a single point which is sometimes referred as point attractor. Existence of non-linearities in the system is the necessary condition for chaotic motion. For a static problem, non-linearity is generated by several possible equilibrium configurations of the system which also modify its dynamics. The complexity in the motion of the system is the result of these conflicts in equilibrium configurations which may lead to chaotic motion.

Sensitivity to initial conditions is a characteristic of chaotic behaviour. This uncertain behaviour forces the engineers not to use the established deterministic approaches towards the solution of some of non-linear problems and instead handle them in a probabilistic approach even if the system parameters are all deterministic [16].

Symonds and Yu [4] studied an elastic-perfectly-plastic beam under short duration pulse loading (impulsive loading),

and showed that final permanent deflection may be in the direction opposite to that of load for certain ranges of input parameters. The numerical solution was carried out by seven finite element and two finite difference codes and surprisingly all codes predicated different responses for the same peak load amplitude which implies the problem is very sensitive to the input parameters as well as rendering the capability of an FE code to simulate these kinds of problems dubious. Forrestal et al. [17] reported on counter-intuitive phenomenon for an elastic-plastic ring subjected to radial pulse pressure loading in which for certain ranges of pulse pressure, the final deflection of the ring rests in the opposite direction of the pulse loading. Experimental results by Ross et al. [18] demonstrated considerable rebound of a fully clamped thin beam when subjected to an impulsive pressure load, which also showed that parts of the beam beside its mid-span may come to rest in the opposite direction of the applied loading and it was concluded that it is difficult to give reasons why the observed response was anomalous or counter-intuitive and hence it is not easy to render suitable the conditions in laboratory to ensure similar results are produced. The predication of existence of counter-intuitive phenomenon in Ref. [4] was supported strongly by experiments in Refs. [9-15, 17-20]. Bassi et al. [10] demonstrated the existence of anomalous response in circular plates with fully fixed boundary and nonlinear elastic, perfect-plastic behaviour by using finite element code ABAQUS and by Galerkin models for one, two, three and eight degrees of freedom.

Based on Symonds's work [4], Q.M. Li and his co-workers [5] studied circular rings subjected to axisymmetric internal pressure pulse assuming elastic, linear plastic kinematic hardening behaviour and it was shown that the counter-intuitive response observed by Forrestal et al. [17] is due to the combined effects of plastic energy dissipation and the kinematic hardening of the ring material, which is totally different from the one responsible for the counter-intuitive responses observed in beams and plates. The result showed that counter-intuitive response can only be expected when hardening modulus is less than half of Young's modulus and when the initial peak strain is in the range of counter-intuitive region and unlike elastic-plastic beam, in which the counter-intuitive region of the loading parameter is normally very narrow and appears and disappears abruptly, counter-intuitive regions for breathing mode response of a ring made of elastic, linear plastic kinematic hardening material are continuous and are not sensitive to the loading parameters. E.A. Flores-Johnson and Q.M. Li [21] conducted a series of numerical studies on the existence of counter-intuitive response in square plates subjected to impulsive loading and map for counter-intuitive region is defined by a non-dimensional number. The asymmetrical response for square plates is also reported in the same work by introducing a small misalignment in full model of the plate.

## 2. Problem definition

In this paper, prototype SDOF and MDOF systems with

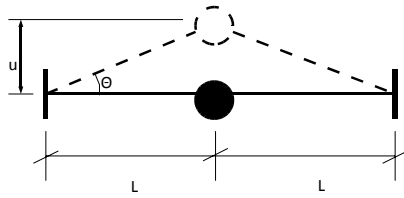


Fig. 1. Taut string.

non-linear resistance functions representing a wide class of structures are studied. As for a SDOF model the lumped mass taut string shown in Fig. 1 (adopted from Ref. [22]) has been studied. SDOF models are simplified versions of continuous structures in which first mode of vibration are the dominant mode and is normally responsible for overall structural failure. Displacement of a SDOF system corresponds to displacement of the real structure at some important point for example the tip of a cantilever beam or midpoint of a plate subjected to impact loading [23] whereas MDOF systems are more realistic representations of various dynamical systems with several significant vibration modes present in the response.

The organization of the work is as follows:

(1) In the first part of this work, a non-linear SDOF system is subjected first to transient and then to periodic loadings. In the governing equation of motion for the system shown in Fig. 1 a quantic term has been included together with the usual cubic term. This ensures more of the nonlinearity has been incorporated into the model. Chaos has been detected by extracting phase space portrait of the solution and calculating Lyapunov's exponent. A similar study is carried out for 2DOF system of nonlinear springs.

(2) In the second part, a SDOF system is studied with elastic-perfectly plastic and elastic-plastic hardening characteristic behaviours.

(3) In the third part, sensitivity to the ratio of initial stiffness to post-yielding stiffness of elastic plastic softening SDOF systems is studied.

(4) The last part consists of dynamic simulations of blast loaded plates and rings using finite element package ABAQUS/CAE 6.9-1 to verify the existence of counter-intuitive response in some simple structural elements and to show that the counter-intuitive windows of parameters for elastic-perfect plastic and elastic plastic kinematic hardening are totally different.

## 2.1 Analytical modelling and response predication

### 2.1.1 Analytical model (SDOF model)

The equation of motion for a damped nonlinear system with odd degree physical nonlinearities up to the fifth order (e.g. as of the system shown in Fig. 1) is the following second order differential equation (Eq. (1))

$$m\ddot{u} + C\dot{u} + k_1u + k_3u^3 - k_5u^5 = P(t) \quad (1)$$

where the over dot denotes differentiation with respect to the

time. The equation of motion is obtained by applying the dynamic equilibrium to the system shown in Fig. 1 as following

$$P(t) - 2T\sin\theta = m\ddot{u} \quad (2)$$

considering

$$\sin\theta = u/(L^2 + u^2)^{\frac{1}{2}} \quad (3)$$

and also

$$T = T_0 + (AE/L)\delta \quad (4)$$

and

$$\delta = (L^2 + u^2)^{\frac{1}{2}} - L. \quad (5)$$

And ignoring terms of higher order than 5 in the expansion of  $\delta$ , the following differential equation is obtained (Eq. (6))

$$\begin{aligned} m\ddot{u} + c\dot{u} + (2T_0/L)u + (AE/L^3)u^3 \\ - (AE/4L^5)u^5 \\ = P(t) \end{aligned} \quad (6)$$

Finally, substituting  $k_1$ ,  $k_3$  and  $k_5$  as a co-efficient for linear, cubic, and quantic terms in the Eq. (6) yields Eq. (1) where

$$k_1 = 2T_0/L \quad (7)$$

if

$$T_0 = 0 \quad (8)$$

Then

$$k_1 = 0. \quad (9)$$

In that case the nondimensionalization should be done by using any other parameter.

$$k_3 = AE/L^3 \quad (10)$$

$$k_5 = AE/4L^5 \quad (11)$$

In non-dimensional form, Eq. (6) can be written as

$$\begin{aligned} d^2v/d\tau^2 + \alpha dv/d\tau + v + \beta(v^3 - \frac{v^5}{4}) \\ = \eta f(\tau) \end{aligned} \quad (12)$$

where the following non-dimensional parameters are introduced to derive Eq. (12)

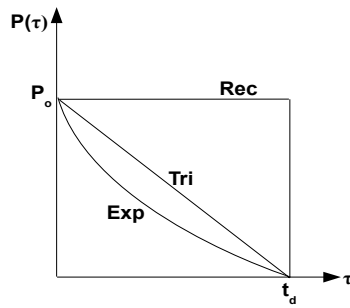


Fig. 2. Rectangular, triangular, and exponential loading time histories, typical of high explosive detonation.

$$v = u/L \quad (13)$$

$$\tau = t/\sqrt{m/k_1} \quad (14)$$

$$\alpha = C/\sqrt{k_1 m} \quad (15)$$

$$\eta = P_0/k_1 L \quad (16)$$

$$\beta = EA/k_1 L \quad (17)$$

where  $L$  is some characteristic length of the problem under consideration e.g. the side of a square plate or the radius of a circular plate. The non-dimensional Eq. (12) has been solved numerically by employing the fourth order Runge Kutta (RK-4) method in MATLAB [24] using ode45 for transient and periodic loadings.

## 2.1.2 Response prediction

### 2.1.2.1 Response under Transient Loading (SDOF model)

In this part, a nonlinear system with cubic and quintic nonlinearities is subjected to pulse load  $P(\tau)$  starting with the maximum value of  $P_0$  and then descending to zero over a period of time with the duration of  $\tau_d$  as it represents a typical detonation process when neglecting the negative phase. The transient loading with rectangular i.e. constant load then a sudden drop at  $\tau_d$ , triangular i.e. linear decay in  $\tau_d$  or exponentially decaying pulse shapes can be expressed using the general expression introduced by Li and Meng [25] and shown in Fig. 2.

$$P(\tau) = P_0(1 - \lambda \tau/\tau_d) \exp(-\gamma \tau/\tau_d) \quad 0 \leq \tau \leq \tau_d \quad (18)$$

$$P(\tau) = 0 \quad \tau > \tau_d \quad (19)$$

Eq. (12) is solved numerically with initial conditions given in Eqs. (20) and (21), and the results are shown in Figs. 3 to 8 for triangular, rectangular and exponential pulses, respectively.

$$v(0) = 0 \quad (20)$$

$$\dot{v}(0) = 0 \quad (21)$$

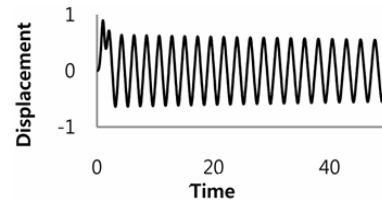


Fig. 3. Time history under triangular pulse.

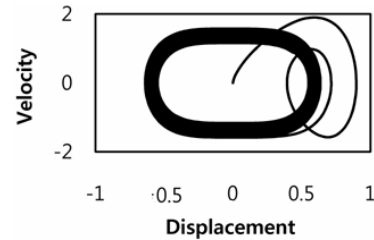


Fig. 4. Phase space portrait under triangular pulse.

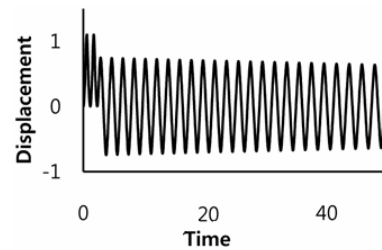


Fig. 5. Time history under rectangular pulse.

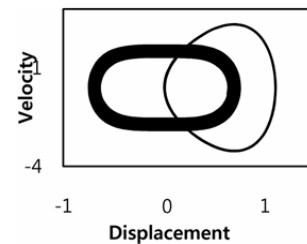


Fig. 6. Phase space portrait under rectangular pulse.

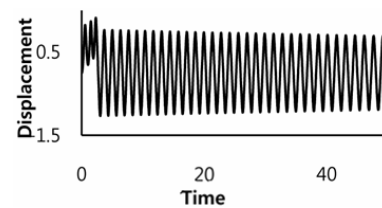


Fig. 7. Time history under exponential pulse.

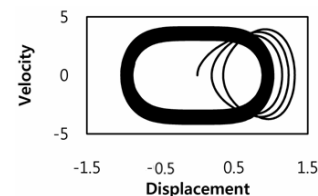


Fig. 8. Phase space portrait under exponential pulse.

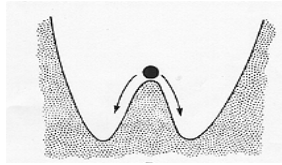


Fig. 9. Two-well potential problem.

From the above response history along with corresponding phase space portrait, one can clearly see that there is no chaos in the response under transient loading. All the responses show a particular pattern in general, with first phase depending upon pulse shape and then the attractor settles down towards a single point when the vibration is damped out gradually.

### 2.1.2.2 Response under periodic loading (SDOF model)

Chaos can be observed qualitatively when the system shown in Fig. 1 is subjected to periodic loading. This chaos is in the form of a two-well potential problem (stability problem) where a ball can go towards left or right of the well when subjected to a small perturbation as shown in the Fig. 9.

To find the ranges of forcing frequencies and forcing amplitudes for the system under study, extensive numerical simulations were carried out by assuming  $\beta = 30$  for coefficient of non-linear term which was relevant to the problem under study. So, Eq. (12) becomes

$$\ddot{v} + \dot{v} + 30(v^3 - \frac{v^5}{4}) = \gamma \cos \omega \tau. \quad (22)$$

A study similar to that of T. Fang E.H Dowell [26] on Duffing's equation and of F. Benedettini and G. Rega [13] on elastic cables with quadratic and cubic non-linearities is carried out for the system under study with cubic and quintic non-linearities. Chaos can be detected by observing phase space portraits of a simulation. Typical chaotic phase portrait is shown in Figs. 10 and 11. It can be visually observed that there is no regular or periodic pattern in response which validates the point that, although all the parameters of the system are deterministic yet the response is un-predictable and hence chaotic.

In the numerical solution, forcing amplitude and forcing frequency were varied parametrically ( $\gamma = 0.25$  to  $3.5$  and  $\omega = 0.25$  to  $3.5$ ). It has been observed that the response is chaotic when forcing amplitude is increased from  $0.25$  to  $2$ . Beyond this point the response is periodic. The results are also validated by calculating Lyapunov's exponent.

If one imagines a set of initial conditions within a sphere of radius  $\epsilon$  in the phase space, then the chaotic motions trajectories originating in the sphere will map the sphere into an ellipsoid whose major axis grows as  $d = \epsilon e^{\lambda t}$ , where  $\lambda$  is known as Lyapunov's exponent. For regular motion  $\lambda \leq 0$ , whereas for chaotic motion  $\lambda > 0$ . Lyapunov's exponents are calculated in MATLAB for a few pairs of forcing amplitude and forcing frequencies and are presented in the Table 1. The Lyapunov's

Table 1. Lyapunov's exponents for SDOF.

$\Omega$ (forcing frequency)	$f$ (forcing amplitude)	Lyapunov's exponent
1	1.2	0.1949
1	1.3	0.1834
1	1.6	0.0617
1.1	1.7	-0.0361
1.2	1.9	0.0173
1.3	2.1	-0.029
1.3	2.5	-0.139
1.4	2.6	-0.3246
1.5	1.7	-0.0362
1.7	2.5	-0.1396

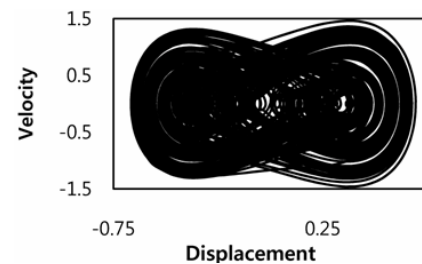
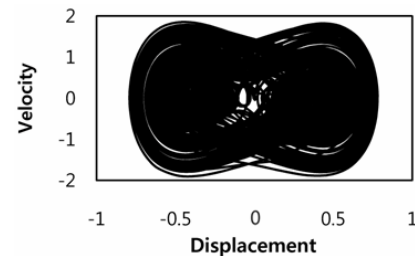
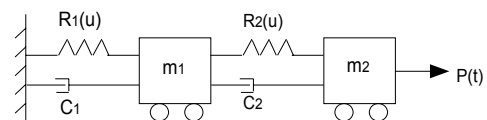
Fig. 10. Phase portrait (for  $\gamma = 1.7$ ,  $\omega = 1.1$ ).Fig. 11. Phase portrait (for  $\gamma = 1.7$ ,  $\omega = 1.1$ ).

Fig. 12. Two degree of freedom system.

exponent is calculated using the algorithm given in Ref. [27].

### 2.1.2.3 Response under periodic loading (MDOF model)

For the sake of completeness a similar study to the one presented in the previous section is carried out for the multi-degree-of-freedom system shown in Fig. 12 which consists of two masses attached to each other and to a fixed boundary through non-linear springs with the outer mass being subjected to the simplest form of periodic loading (a simple harmonic). The reason for the choice of two degrees of freedom is that a 2DOF system replicates all the important results an MDOF system can generate and all fundamental features of MDOF systems can be explained using a 2DOF system.

The equations of motion for the MDOF system shown in Fig. 12 are given by Eqs. (23) and (24) as follows:

$$m_1 \ddot{u}_1 + 2C_1 \dot{u}_1 - C_2 \dot{u}_2 + 2k_1 u_1 - k_1 u_2 + k_3 u_1^3 - k_5 u_1^5 - k_3 (u_2 - u_1)^3 + k_5 (u_2 - u_1)^5 = 0 \quad (23)$$

$$m_2 \ddot{u}_2 + C_2 \dot{u}_2 - C_2 \dot{u}_1 + k_1 u_2 - k_1 u_1 + k_3 (u_2 - u_1)^3 - k_5 (u_2 - u_1)^5 = P(t) \quad (24)$$

where  $m_1$ ,  $m_2$  designate masses,  $C_1$ ,  $C_2$  are the damping coefficients, and  $k_1, k_2, k_3, k_5$  are the stiffness coefficients for first and second degrees of freedom in the model. This means we postulate the stiffness coefficients for the springs to be the same while masses and damping coefficients are different for the two degrees of freedom. This reduces the level of complexity in the model and renders the analyses for discerning chaotic behaviour easier to conduct. Using the non-dimensional parameters introduced in the previous section, Eqs. (27) and (28) reduce to

$$\ddot{v}_1 + \alpha(2\dot{v}_1 - \dot{v}_2) + 2v_1 - v_2 + \beta v_1^3 - \beta v_1^5/4 - \beta(v_2 - v_1)^3 + \beta(v_2 - v_1)^5/4 = 0 \quad (25)$$

$$\ddot{v}_2 + \alpha(\dot{v}_2 - \dot{v}_1) + v_2 - v_1 + \alpha(v_2 - v_1)^3 - \beta(v_2 - v_1)^5/4 = \eta f(t). \quad (26)$$

For the 2DOF model, a similar study is conducted as in previous section for SDOF. The system is considered to be undamped and hence  $C_1$  and  $C_2$  both are equal to zero. A parametric study was carried out and the equations of motion were solved numerically in MATLAB using Runge-Kutta method of order 4. In Eqs. (25) and (26) forcing amplitude and forcing frequency were varied from 0.25 to 3.5. For the 2DOF system, the chaotic regime is very different than single degree of freedom systems. The response is chaotic for the values of forcing amplitudes between 0 and 1.75 beyond which the response becomes periodic. On the other hand, the response is independent of forcing frequency for these particular combinations of frequencies and amplitudes. Some phase portraits along with displacement histories are shown in the Fig. 13-20. Lyapunov exponents are also calculated for a few pairs of frequencies and amplitudes and are given in the Table. 2. Where positive maximum Lyapunov exponent is the indication of chaotic motion.

#### 2.1.2.4 Chaos in SDOF systems with elastic-perfectly-plastic and elastic-plastic-hardening resistance elements

In this part, the prototype non-linear SDOF system as

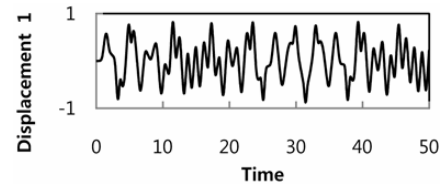


Fig. 13. Displacement history 1<sup>st</sup> degree (for  $\gamma = 1.7$ ,  $\omega = 1.1$ ).

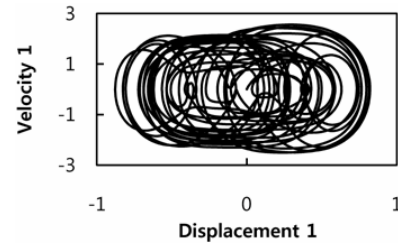


Fig. 14. Phase portrait 1<sup>st</sup> degree (for  $\gamma = 1.7$ ,  $\omega = 1.1$ ).

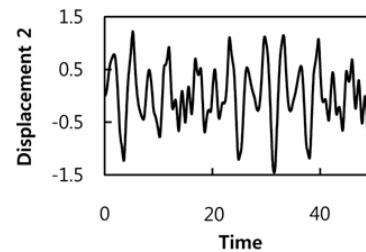


Fig. 15. Displacement history 2<sup>nd</sup> degree (for  $\gamma = 1.7$ ,  $\omega = 1.1$ ).

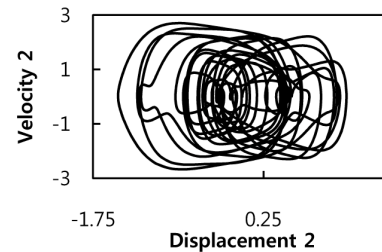


Fig. 16. Phase portrait 2<sup>nd</sup> degree (for  $\gamma = 1.7$ ,  $\omega = 1.1$ ).

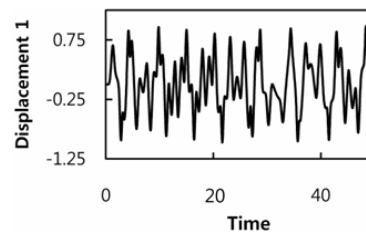


Fig. 17. Displacement history 1<sup>st</sup> degree (for  $\gamma = 2.6$ ,  $\omega = 1.3$ ).

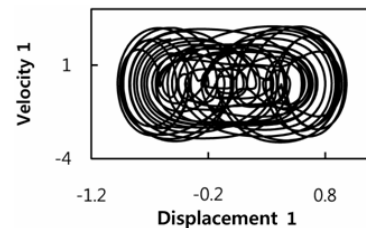


Fig. 18. Phase portrait 1<sup>st</sup> degree (for  $\gamma = 2.6$ ,  $\omega = 1.3$ ).



Table 2. Lyapunov's exponents for MDOF.

$\Omega$ (forcing frequency)	F (forcing amplitude)	Lyapunov's exponent
1	1.2	-0.7514
1	1.3	-0.5815
1	1.6	-0.4119
1.1	1.7	-0.3356
1.2	1.9	-0.1414
1.3	2.1	0.4569
1.3	2.5	1.368
1.4	2.6	1.5795
1.5	1.7	-0.3338
1.7	2.5	1.3571

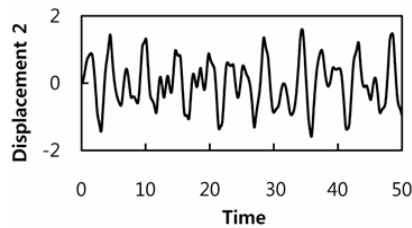
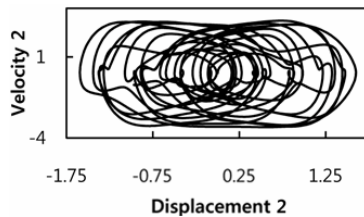
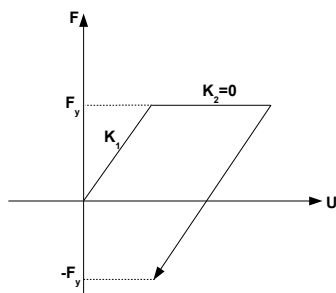
Fig. 19. Displacement history 2<sup>nd</sup> degree (for  $\gamma = 2.6$ ,  $\omega = 1.3$ ).Fig. 20. Phase portrait 2<sup>nd</sup> degree (for  $\gamma = 2.6$ ,  $\omega = 1.3$ ).

Fig. 21. Elastic, perfectly plastic behaviour.

shown in Fig. 1, is studied but with elastic-perfect-plastic and elastic-plastic-hardening behaviour. For simplicity the system is assumed un-damped, nonetheless; this will not affect the type of behaviour expected.

#### 2.1.2.4.1 Response of the elastic-perfectly-plastic system

For an un-damped elastic-perfectly-plastic system, the equation of motion is as follows:

$$\ddot{u} + r(u) = P(t) \quad (27)$$

With the resistance function  $r(u)$  being defined in Fig. 21. The slope of resistance curve is defined as

$$\begin{aligned} k &= k_1 \text{ if } |r(u)| < F_y \\ k &= k_1 \text{ if } |r(u)| = F_y \text{ and } r(u) \cdot \dot{u} < 0 \\ k &= k_2 \text{ if } |r(u)| = F_y \text{ and } r(u) \cdot \dot{u} > 0. \end{aligned} \quad (28)$$

In the non-dimensional form, the above equation is written as

$$\ddot{v} + r(\tau) = f(\tau) \quad (29)$$

Li and Liu [6] have studied the sensitivity of parameters involved in the counter-institutive phenomenon encountered in elastic-plastic beam dynamics. The analytical model used in Ref. [6] consists of a sandwich beams with two deformable flanges (unit cell being called a Shanley cell). The flanges of Shanley cell can only sustain uniaxial load and are able to produce both membrane and bending resistances. This implies that a Shanley-type model is able to represent a beam when the transverse shear deformation is not significant and thus negligible. In order to simplify the analysis in Ref. [6] it is assumed that the pulse loading on the model is short and intensive so that the maximum displacement is reached prior to the pulse loading being completed. This assumption implies that the recovery response phase of the model is determined only by the maximum displacement or the maximum rotation angle, and therefore, the external loading can be replaced by an initial rotation angle and hence it has been assumed that  $f(\tau) = 0$ , and  $\dot{v}_0 = 0$ .

The equation used in Ref. [6] is of the following form

$$\ddot{v} + kv = F \quad (30)$$

The values of  $k$  and  $F$  depend upon the stress states in the upper and lower flanges of the beam in the analytical model.

The above Eq. (30) has been solved numerically using Newmark- $\beta$  [28] with  $\beta = 1/4$  and  $\gamma = 1/2$  in Matlab using an algorithm given in Ref. [29] and with different initial values of displacements. For a very narrow range of initial displacement, the response is counter-intuitive. In all cases initial velocity is zero.

$$\dot{v}(0) = 0. \quad (31)$$

The response is shown in the Figs. 22-24 and it can be seen that when  $\Phi = 0.09$ , the response is counter-intuitive.

#### 2.1.2.4.2 Response of elastic-plastic-hardening system under transient loading

In this part an SDOF system with bilinear elastic plastic kinematic hardening is studied. The elastic plastic hardening

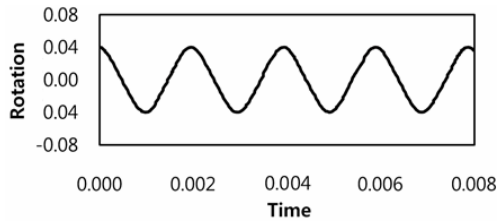
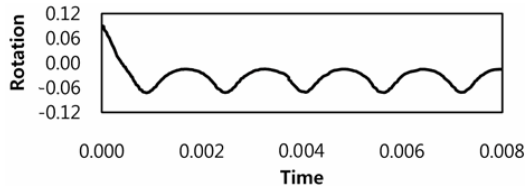
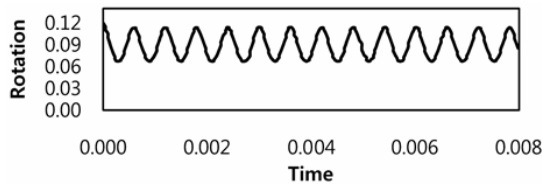
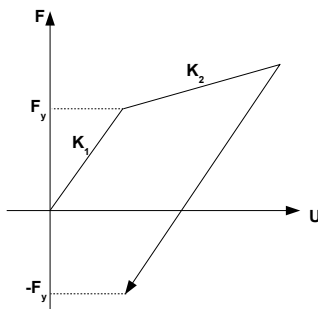
Fig. 22. Response for initial angle  $\Phi = 0.04$ .Fig. 23. Response for initial angle  $\Phi = 0.09$ .Fig. 24. Response for initial angle  $\Phi = 0.12$ .

Fig. 25. Elastic linear plastic, kinematic hardening behaviour.

relationship is shown in Fig. 25.

The equation of motion for this case remains the same as that of the previous case.

$$\ddot{u} + r(u) = P(t) \quad (32)$$

The initial conditions are:

$$u(0) = 0 \quad (33)$$

$$\dot{u}(0) = 0 \quad (34)$$

The counter-intuitive phenomenon in such an SDOF system has been observed in Ref. [5] when a circular ring is subjected to triangular pressure pulse of different amplitudes. The counter-intuitive phenomenon in this case is different from the

one observed in elastic plastic beams and plates where it only occurs in narrow ranges of amplitude and disappear abruptly which renders those problems highly parametric sensitive. The counter-intuitive phenomenon in this case is based on breathing mode response of a circular ring and regions of counter-intuitive response are continuous and are not sensitive to the loading parameters. According to Ref. [5], the counter-intuitive response will not happen in bilinear elastic-plastic kinematic hardening material when its hardening modulus is greater than or equal to half of its Young's modulus, in elastic-perfectly-plastic material or in bilinear elastic plastic isotropic hardening material. These observations are based on energy method and have been explained in Ref. [5]. The equation of motion for a single degree of freedom system in radial direction for different stages of response is given as:

$$\rho h a \frac{d^2 w}{dt^2} + h \sigma = a p(t) \quad (35)$$

Here in this case, only triangular loading has been considered. As in Ref. [5], the equation of motion is written for a thin plane-strain ring. Hook's law for the plane-strain is

$$\sigma = \frac{E}{1 - \nu^2} \varepsilon = \frac{E}{1 - \nu^2} \frac{w}{a} \quad (36)$$

Combining the two equations gives

$$\frac{d^2 \varepsilon}{dt^2} + \delta^2 \varepsilon = \frac{p(t)}{\rho a h} \quad (37)$$

where  $\delta$  is given as

$$\delta = \sqrt{\frac{E}{\rho a^2 (1 - \nu^2)}} \quad (38)$$

The solution of Eq. (35) gives the elastic part of response. For plastic part, the equation is modified for plastic loading response stage and reversed elastic and plastic loading response stages. These equations are given in detail in Ref. [5] and are the basis of simulations for elastic, plastic kinematic hardening circular ring carried out in the last part of the present paper.

### 2.1.3 Sensitivity studies for an elastic-plastic-softening system

In this part, a sensitivity study has been carried out for an elastic plastic softening system subjected to rectangular pulse load only. The resistance function used here is shown in the Fig. 26.

In the non-dimensional form, the equation of motion which is the same as in Ref. [23] for elastic-plastic softening case is written as,



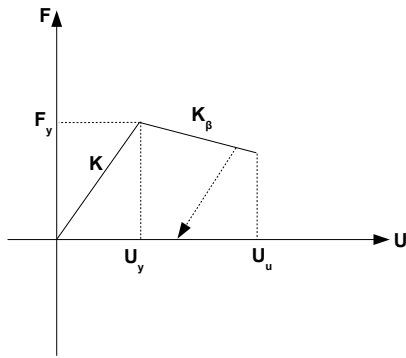


Fig. 26. Elastic, linear plastic kinematic softening behaviour.

For elastic range:

$$\ddot{v} + v = pf(\tau) \quad (39)$$

For plastic softening range:

$$\ddot{v} - \psi^2 v = pf(\tau) - (1 + \psi^2)\alpha \quad (40)$$

where

$$\psi = \sqrt{k_\beta/k} \quad (41)$$

Solving the above equation with initial condition

$$v(0) = 0 \quad (42)$$

$$\dot{v}(0) = 0 \quad (43)$$

Here the most general case has been assumed in which plasticity begins before  $\tau_d$  (where  $\tau_d$  is the dimensionless load duration). Displacements are computed analytically for two plastic regimes, i.e. first for forced vibrations (i.e. after  $\tau_e$  and before  $\tau_d$ ) and second for free vibrations (i.e. after  $\tau_d$ ). These equations are solved in Maple [30] to find time corresponding to maximum displacement.

Then sensitivity to parameter  $\psi$  has also been studied and shown in Figs. 27 and 28. For realistic values of  $k_\beta$  and  $k$ , non-dimensional parameter,  $\psi$  varies between 0.1 and 0.8. Where the value of 0.1 indicates the case in which  $k_\beta$  is 10% of  $k$  (the lower bound) and 0.8 (the upper limit) indicates  $k_\beta$  as 80% of  $k$ . From Figs. 27 and 28, it is clear that maximum displacement increases as the ratio between initial stiffness and post-yielding or plastic stiffness (softening in this case) increases up to a certain range and then start decreasing afterwards for both Phase 1 and Phase 2.

## 2.2 ABAQUS/CAE 6.9-1 simulation results

### 2.2.1 Elastic, perfectly plastic systems

To show the existence of counter-intuitive in a simple structural element, some examples are adopted and ABAQUS/CAE 6.9-1 [31] simulations are carried out. The first example con-

Table 3. Simulation parameters for rectangular plate.

Length (mm)	300
Width (mm)	300
Thickness (mm)	4
E (GPa)	80
$\sigma_0$ (MPa)	300
$\rho$ (kg/m <sup>3</sup> )	2700
$\nu$	0.3
$t_d$ (ms)	0.5

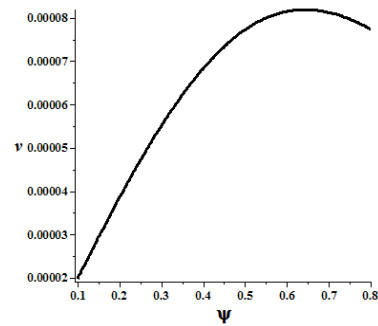


Fig. 27. Sensitivity of maximum displacement to stiffness Ratio for Phase 1 (forced vibrations).

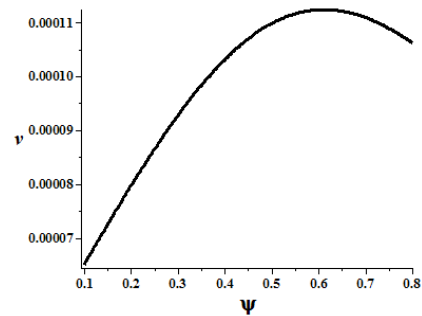


Fig. 28. Sensitivity of maximum displacement to stiffness Ratio for Phase 2 (forced plastic vibrations).

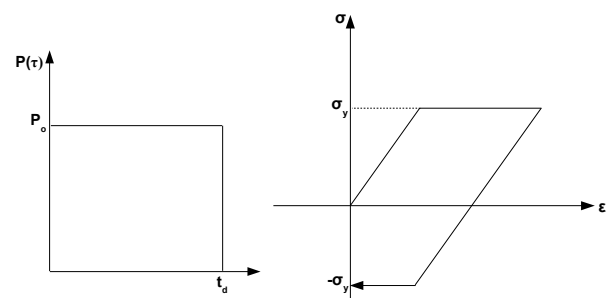


Fig. 29. Pulse shape and elastic perfectly plastic stress strain relation.

sists of a rectangular plate with pinned-ended constraints. The plate dimensions and material properties are shown in Table 3.

Here it is important to mention that the material properties and the pulse shape with duration equal to 0.5 msec, are taken from Ref. [7]. The plate is modelled in ABAQUS using a

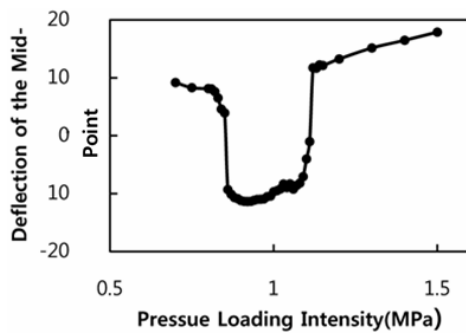


Fig. 30. Variation of final mid-point displacement with loading intensity ( $p_0$ ).

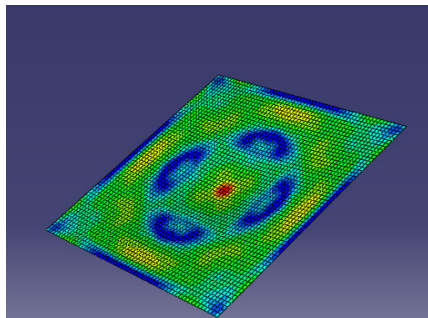


Fig. 31. Finite element model of the plate in ABAQUS/CAE 6.9-1.

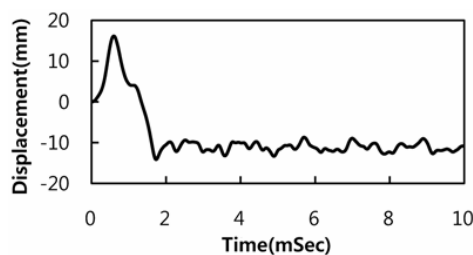


Fig. 32. Displacement time history of mid-point of the plate under impact loading ( $p_0 = 0.95$  MPa).

general purpose shell element i.e. S4R which is a 4-noded doubly curved thin or thick shell, with reduced integration, hourglass controlled capable to capture finite membrane strains. The material of the plate is elastic-perfect-plastic. Counter-intuitive response was obtained for different ranges of loading parameters. The counter-intuitive window obtained in this example is slightly wider than that given in Ref. [7]. Counter-intuitive response is obtained when  $0.86 \text{ MPa} < p_0 < 1.12 \text{ MPa}$  and the width of the window is less than  $0.26 \text{ MPa}$ . The results are deterministic as long as the system parameters and computation parameters are fixed and results are repeatable as also shown in Ref. [7]. But the change in computation parameter e.g. element type or FE software might change the location of counter-institutive window or might influence the existence of the counter-intuitive or anomalous response. The variation in average deflection during final elastic vibration phase for an elastic-plastic rectangular plate against the pressure magnitude is shown in Fig. 30.

Table 4. Simulation parameters for circular plate.

Radius (mm)	300
Thickness (mm)	300
E (GPa)	70
$\sigma_0$ (MPa)	300
$\rho$ (kg/m <sup>3</sup> )	2700
$\nu$	0.35
$t_d$ (ms)	0.2

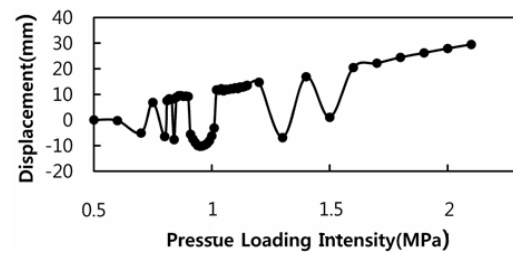


Fig. 33. Variation of final mid-point deflection with loading intensity  $p_0$ .

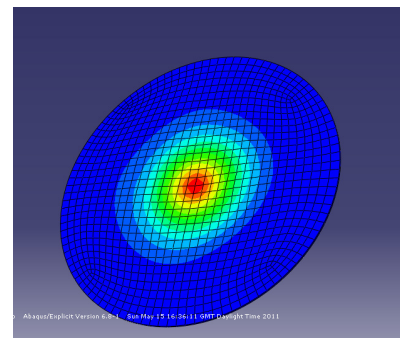


Fig. 34. Finite element model of the circular plate in ABAQUS/CAE 6.9-1.

A typical counter-intuitive response of the mid-point deflection of the studied plate which is obtained from ABAQUS/CAE 6.9-1 simulation for  $p_0 = 0.95 \text{ MPa}$  is shown in Fig. 32.

The second example consists of a circular plate having elastic, perfectly plastic behaviour with fixed boundaries. The plate dimensions and material properties are shown in Fig. 4.

The plate is subjected to rectangular pulse with  $t_d = 0.2 \text{ msec}$  and is modelled in ABAQUS using general purpose shell elements. The counter-intuitive window in this case is very irregular, especially during transition from purely elastic response to mixed elastic and plastic response. To search for counter-intuitive window in terms of magnitude of pressure, 50 simulations were carried out by increasing the pressure magnitude gradually in each simulation. A very irregular response was observed which is shown in Fig. 33.

A typical displacement time history of central point of the plate in transverse direction is shown in the Fig. 34. Hence it is found that unlike rectangular plate, the counter-intuitive

Table 5. Dimensions and material parameters for Ring-1.

Radius of the centre line (mm)	41
Thickness (mm)	2
E (GPa)	200
$E^t$ (GPa)	50
$\sigma_0$ (MPa)	200
$\rho$ (kg/m <sup>3</sup> )	7830
$\nu$	0.3

Table 6. Dimensions and material parameters for Ring-2.

Radius of the centre line (mm)	41
Thickness (mm)	2
E (GPa)	200
$E^t$ (GPa)	100
$\sigma_0$ (MPa)	200
$\rho$ (kg/m <sup>3</sup> )	7830
$\nu$	0.3

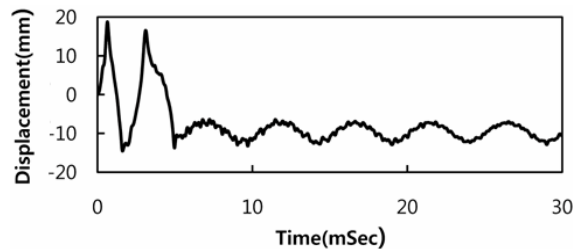


Fig. 35. Displacement time of central point of the plate in transverse direction.

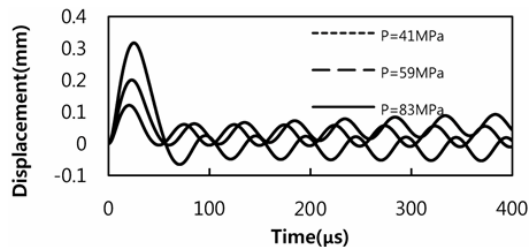


Fig. 36. Displacement time history of a midpoint for Ring-1.

window for circular plate is very random during the transition from elastic to mixed elastic plastic responses. This implies a phenomenon which can be termed as “second order chaos” where not only the response is chaotic but also the response direction ranges follow chaos.

### 2.2.2 Elastic-plastic, kinematic hardening systems

In this part of the work, simulations were carried out using Abaqus/CAE 6.9-1 for a ring type structure to validate the presence of counter-intuitive response for elastic plastic kinematic hardening material behaviour. The ring dimensions are the same as given in Ref. [5] and also presented in Table 5 and

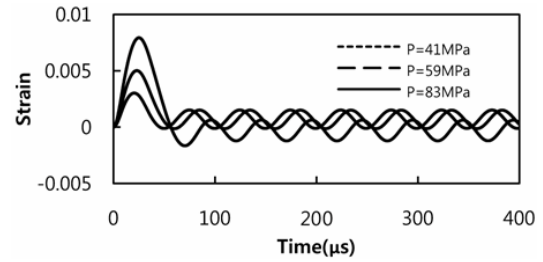


Fig. 37. Strain time history for Ring-1.

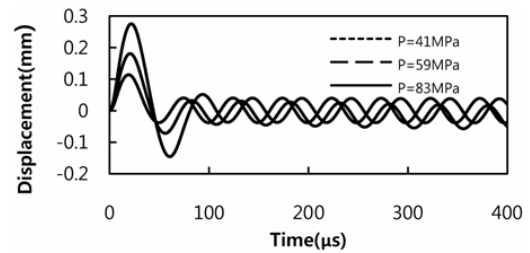


Fig. 38. Displacement time history of a midpoint of Ring-2.

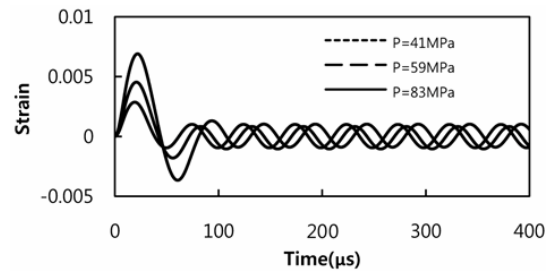


Fig. 39. Strain time history for Ring-2.

Table 6. Full ring has been modelled and is subjected to triangular pressure pulse with duration of 10  $\mu$ s. For Ring 1 whose tangent modulus is less than the one half of Young's modulus counter-intuitive response is obtained. The displacement and strain time histories are shown in the Figs. 36-39. This displacement is in the radial direction.

### 3. Conclusions

In this paper counter-intuitive or chaotic response of SDOF as well as MDOF systems with different resistance characteristics is studied. Following conclusions can be drawn from this study.

(1) In large deformation problems, with cubic and quantic non-linearity, there is no chaos when the system is subjected to transient loading.

(2) The behaviour of the SDOF and MDOF system with cubic and quantic non-linearity is chaotic for certain ranges of forcing frequencies and forcing amplitudes when the system is subject to periodic loading. Therefore, for designing systems subjected to periodic loading such as structures with mounted electric machines etc, careful study of the system must be carried out to avoid these uncertain dynamic responses.

(3) For SDOF systems with elastic perfect-plastic material behaviour, when subjected to short duration loading, behaves counter-intuitively for certain ranges for amplitudes.

(4) It is also possible that in some case local counter-intuitive response may be accompanied by large local plastic deformation and hence may lead to local failure of structural component.

(5) For elastic plastic softening systems, maximum response increases as the ratio between initial stiffness and post-yielding or plastic stiffness (softening in this case) increases up in a certain range and then start decreasing afterwards.

(6) The existence of counter-intuitive response is validated by Finite element simulations in ABAQUS/CAE 6.9-1. The results indicate that the determination of window in which counter-intuitive response is expected depends upon the type of structure under consideration. For some structural types it is possible to determine the window in which the response is explicitly counter-intuitive, whereas in others, the ranges are varying, particularly during the transition from elastic to mixed elastic-plastic responses. Also there are some structural types such as circular ring in which the counter-intuitive window is continues.

## Nomenclature

$a$	: Radius of the circular ring
$A$	: String's cross sectional area
$C$	: Damping co-efficient
$E$	: Modulus of elasticity for string material
$F_y$	: Spring force at yielding point
$h$	: Ring height
$k_1$	: Co-efficient of linear stiffness term
$k_3$	: Co-efficient of cubic stiffness term
$k_5$	: Co-efficient of quintic stiffness term
$k_\beta$	: Softening stiffness
$L$	: Length of string
$m$	: Mass of the system
$P_0$	: Loading Amplitude
$r(u)$	: Resistance function
$t$	: Time
$t_d$	: Duration of loading
$T$	: Tension in string
$T_0$	: Initial tension in string
$u$	: Displacement component
$v$	: Non-dimensional displacement
$w$	: Radial displacement in ring
$\theta$	: Angle between initial & displaced position of string
$\lambda$	: Loading shape parameter
$\gamma$	: Loading shape parameter
$\rho$	: Density
$\psi$	: Ratio of post yield stiffness to initial stiffness
$\varepsilon$	: Strain
$\alpha$	: Non-dimensional parameter
$\beta$	: Non-dimensional parameter
$\delta$	: Non-dimensional parameter

$\eta$	: Non-dimensional parameter
$\omega$	: Excitation frequency

## References

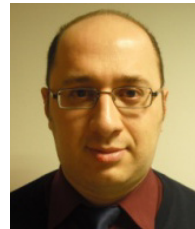
- [1] S. U. Galiev, Experimental observations and discussion of counterintuitive behavior of plates and shallow shells subjected to blast loading, *International Journal of Impact Engineering*, 18 (1996) 783-802.
- [2] S. U. Galiev, Distinctive features of counter-intuitive behavior of plates and shells after removal of impulse load, *International Journal of Impact Engineering*, 19 (1997) 175-87.
- [3] S. U. Galiev, Numerical modeling unexpected behavior of sheets in experiments carried out by M. A. Lavrent'ev, *Strength of Materials*, 25 (1993) 381-6.
- [4] P. S. Symonds and T. X. Yu, Counterintuitive behavior in a problem of elastic-plastic beam dynamics, *Journal of Applied Mechanics*, 52 (1985) 517-22.
- [5] Q. M. Li, Q. Dong and J. Y. Zheng, Counter-intuitive breathing mode response of an elastic-plastic circular ring subjected to axisymmetric internal pressure pulse, *International Journal of Impact Engineering*, 35 (2008) 784-94.
- [6] Q. M. Liu and Y. M. Li, Correlation between parameter sensitivity and counter-intuitive phenomenon of elastic-plastic beam dynamics, *Computers & Structures*, 84 (2006) 156-65.
- [7] Q. M. Li and Y. M. Liu, Uncertain dynamic response of a deterministic elastic-plastic beam, *International Journal of Impact Engineering*, 28 (2003) 643-51.
- [8] Q. M. Li, Y. M. Liu and G. W. Ma, The anomalous region of elastic-plastic beam dynamics, *International Journal of Impact Engineering*, 32 (2006) 1357-69.
- [9] Q. M. Li, L. M. Zhao and G. T. Yang, Experimental results on the counter-intuitive behaviour of thin clamped beams subjected to projectile impact, *International Journal of Impact Engineering*, 11 (1991) 341-8.
- [10] A. Bassi, F. Genna and P. S. Symonds, Anomalous elastic-plastic responses to short pulse loading of circular plates, *International Journal of Impact Engineering*, 28 (2003) 65-91.
- [11] J. Argyris, V. Belubekian, N. Ovakimyan and M. Minasyan, Chaotic vibrations of a nonlinear viscoelastic beam, *Chaos, Solitons & Fractals*, 7 (1996) 151-63.
- [12] L. D. Zavodney, A. H. Nayfeh and N. E. Sanchez, Bifurcations and chaos in parametrically excited single-degree-of-freedom systems, *Nonlinear Dynamics*, 1 (1990) 1-21.
- [13] F. Benedettini and G. Rega, Numerical simulations of chaotic dynamics in a model of an elastic cable, *Nonlinear Dynamics*, 1 (1990) 23-38.
- [14] J. M. T. Thompson, An introduction to nonlinear dynamics, *Applied Mathematical Modelling*, 8 (1984) 157-68.
- [15] N. L. Bruce Henry and F. Camacho, Non-linear dynamic

time series analysis, *Nonlinear biomedical signal processing*, (2001).

- [16] F. Bontempi and F. Casciati, Non-linear dynamics versus chaotic motion for MDOF structural systems, *Chaos, Solitons & Fractals*, 7 (1996) 1659-82.
- [17] M. J. Forrestal, D. Y. Tzout and J. Li, A counterintuitive region of response for elastic-plastic rings loaded with axisymmetric pressure pulses, *International Journal of Impact Engineering*, 15 (1994) 219-23.
- [18] C. A. Ross, W. S. Strickland and R. L. Sierakowski, Response and failure of simple structural elements subjected to blast loadings, *Shock and Vibration Inform*, 9 (1977) 15-26.
- [19] H. Kolsky, P. Rush and P. S. Symonds, Some experimental observations of anomalous response of fully clamped beams, *International Journal of Impact Engineering*, 11 (1991) 445-56.
- [20] F. Genna and P. S. Symonds, Dynamic plastic instabilities in response to short-pulse excitation: Effects of slenderness ratio and damping, proceedings of the royal society of london series A, *Mathematical and Physical Sciences*, 417 (1988) 31-44.
- [21] E. A. Flores-Johnson and Q. M. Li, A brief note on the counter-intuitive region of a square plate, *International Journal of Impact Engineering*, 38, 136-8.
- [22] R. Roy and J. Craig, *Structural dynamics: An introduction to computer methods*, John Wiley & Sons (1981).
- [23] A. S. Fallah and L. A. Louca, Pressure-impulse diagrams for elastic-plastic-hardening and softening single-degree-of-freedom models subjected to blast loading, *International Journal of Impact Engineering*, 34 (2007) 823-42.
- [24] MathWorks, Matlab R2010a, 7.10.0.499(R2010a) ed: The MathWorks (2010).
- [25] Q. M. Li and H. Meng, Pressure-impulse diagram for blast loads based on dimensional analysis and single-degree-of-freedom model, *Journal of Engineering Mechanics*, 128 (2002) 87-92.
- [26] T. Fang and E. H. Dowell, Numerical simulations of periodic and chaotic responses in a stable duffing system, *International Journal of Non-Linear Mechanics*, 22 (1987) 401-25.
- [27] A. Wolf, J. B. Swift, H. L. Swinney and J. A. Vastano, *Determining Lyapunov exponents from a time series*, Physica D: Nonlinear Phenomena, 16 (1985) 285-317.
- [28] N. M. Newmark, A method of computation for structural dynamics, *J Engng Mech Div*, ASCE (1959) 67-94.
- [29] A. K. Chopra, *Dynamics of structures: Theory and applications to earthquake engineering*, 3rd ed: Pearson Prentice Hall (2007).
- [30] Maplesoft, Maple, 14.00 ed: Maplesoft and Maple (2010).
- [31] Dassault Systemes Simulia Corp. P, RI, USA. ABAQUS 6.9.1 ed: Simulia (2009).



**Luke A. Louca** is a Reader in structural engineering in the Department of Civil and Environmental Engineering at Imperial College London. He is engaged in teaching at both undergraduate and postgraduate level in both structural steel design and mitigating the effects of explosions on structures. His principal research interests, where he has published some 40 papers in leading journals and conferences, lie in the areas of behaviour and design of structures subjected to explosions and impact loads. Much of this has focussed on steel structures for offshore applications as well as defence applications using both traditional construction materials and fibre reinforced composite structures. Although much of his work is computational, laboratory testing of small scale specimens is also being conducted under dynamic loading. Large scale testing has also been carried out off-site with a number of sponsors where he has been involved in the design of the tests. Much of the work is funded by the EPSRC, Dstl/MoD, Health and Safety Executive and the Office of Naval Research (USA).



**Arash S. Fallah** is a Research Associate in structural engineering at Imperial College London specialising in computational and analytical modelling of blast and impact loaded monolithic, composite and hybrid structures and systems. His interests include frequency filtering in phononic metamaterials and lattices, extended finite element formulation of plated structures, nonlinear dynamics and chaos, damage and fracture in composites and constitutive visco-elastic, plastic and visco-plastic formulations for metals and composites. Much of his work is funded by EPSRC, Dstl/MoD, Health and Safety Executive and the Office of Naval Research Global and is conducted in collaboration with University of Cape Town and US Naval Academy.



**S. K. A. Shah** received his B.Sc. degree in Civil Engineering from University of Engineering and Technology Peshawar, Pakistan in 2007 and an M.Sc. in Earthquake Engineering from Rose School of Earthquake Engineering, Pavia, Italy in 2009. He is currently a postgraduate Research Student at Imperial College London in structural engineering. His research interests are analysis of blast loaded plates and shells, constitutive modeling of composite materials, evaluation of damage in impact and blast loaded fibre-metal laminates, structural dynamics and chaos and earthquake engineering.